884H1: Topics in Wireless Communications

Project Assignment

Candidate Number: 218831

Due date: 26/05/2019

Contents

Background

The mobile communication systems are one of the constant pillars of human development, first allowing users to communicate with each other using large and inefficient systems compared to what is available today. Each generation of mobile communications comes at the early years of the decade while having at least one revision at the middle of its lifetime; each of these delivers fascinating new features and improvements in both speed and reliability.

As 2G introduced the implementation of digital communications instead of being analog, many other characteristics were to be invented, such as text messages and multimedia messages. This convention is still relevant, as every following generation keeps the use of digital communications.

The goals set to each generation are the driving motivation for engineers to come up with newer and more advanced techniques that makes the most of the available resources. For example, the need of faster data throughput and to support a vast number of users led to the implementation of ODFM as the second modulation technique and the multiple-access scheme of 4G (More about this in the **Wireless Waveforms** section).

The use of mobile communications moved from being a commodity to an increasing necessity since industries now depend on these technologies, and people are used to its inclusion in their lives. The previous statement means that the upcoming generation of mobile communications must support features for the current industries and the newcomers to use the communication infrastructure reliably. This decade's generation, 5G, is already being deployed in some parts of the world and its technical proposal includes several new technologies; some of these are already mature while others still present an engineering challenge.

Some of these technologies are described in the following sections, going from the already known techniques for modulation (**Wireless Waveforms**), message coding for correcting errors in transmission (**Channel Coding**) and multicarrier modulation (**OFDM**) to the application specific techniques such as **Spatial Diversity** and **MIMO**.

Finally, a description of **Beamforming**, a mature technique already used in several other industries, including its theory, mathematical background, use in 5G and simulation.

Wireless Waveforms

As mobile communications evolve, technologies and techniques are updated, affecting characteristics in time and frequency domain. Since the first generation of mobile communications, features like multiplexing/Multiple-Access, modulation, number of carriers (or general bandwidth availability) have been engineering challenges to overcome to offer a service of quality to end-users.

M-PSK

M-ary Phase Shift Keying is a form of single-carrier, phase modulated, constant amplitude modulation scheme in which the input signal is coded into a correlated sinewave with variable phase. The number of possible phase angles is defined by the M-ary number (M), this number also represents the name of the modulation scheme and the number of bits per symbol (k) at the modulated signal.

$$k = \log_2 M$$
$$M = 2^k$$

Equation 1. Relationship between the M-ary number (M) and the number of bits per symbol (k).

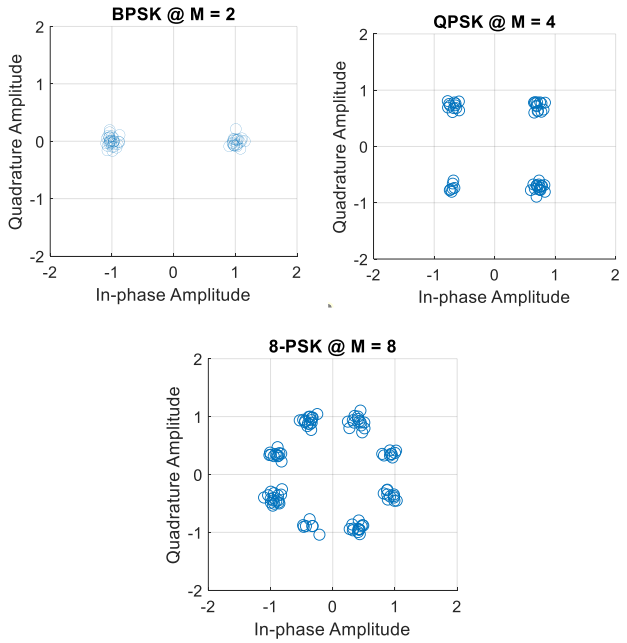

Figure 1. Various M-PSK constellation diagrams.

M-QAM

Quadrature Amplitude Modulation is a Single-Carrier form of modulation like M-PSK in which both amplitude and phase are used to code the input signal. In QAM, amplitude levels and phase angles are meant to create square-shaped constellations (although non-square constellations are used, as well). The main performance difference between QAM and PSK is the spatial distance between constellation points which is (roughly saying) proportional to Bit Error Performance (BER), making QAM more error robust at the cost of power efficiency.

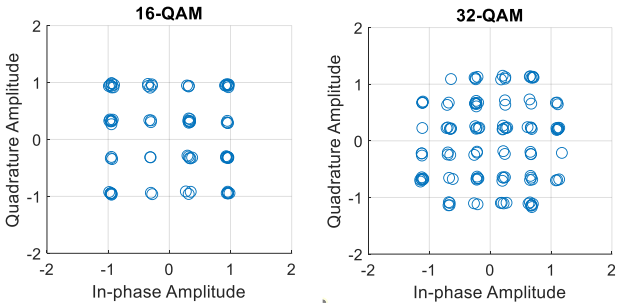

Figure 2. Various M-QAM constellation diagrams.

OFDM

Orthogonal Frequency Division Multiplexing is the multiplexing (and Multiple Access) technique used in 4G systems. OFDM is a multicarrier technique with several advantages to single carrier modulation being fading robustness and bandwidth efficiency the main features of it.

As its name implies, OFDM uses the orthogonality property to place sub-carriers close to each other in the frequency domain without overlapping, increasing the bandwidth efficiency abruptly. The Sub-Carrier's bandwidth is used as the Sub-Carrier spacing and its inverse as the symbol time.

Practical applications of OFDM implement FFT/IFFT to combine all the different subcarriers into a single time-domain signal (To avoid using multiple oscillators) and a so-called "Cycle-Prefix" as guard-interval between symbols to avoid shifts in the frequency domain and Inter-Symbol Interference

The number of subcarriers is given by the next higher power of two that results in more than the required subcarriers to meet the design goals.

$$N_{sub-carriers} = 2^n > N_{required-SC}, n = 1, 2, 3, \ldots$$

Ideally, every subcarrier should be used to carry user data, but some of them are used as pilots (a known signal used for channel estimation), guard-band or simply not used (such as the DC null carrier). Designers can decide on how sub-carriers are allocated, affecting the overall efficiency of the system.

OFDM is often represented as a grid of "Resource Elements", each one representing a Sub-Carrier in both time and frequency domains.

MATLAB's Wireless Waveform Generator App helps to create various kinds of modulated signals (as shown in Figure 2 and Figure 3). An OFDM waveform was generated using the following parameters using MATLAB.

Parameter	**Value**
FFT Length	64
Guard Band Sub-Carriers	6 and 5
DC Null	No
Cyclic Prefix Length	16
OFDM Symbols	100
Sub-Carrier Spacing	1 MHz
Pilot Input	No

Table 1. Parameter table for OFDM waveform (a).

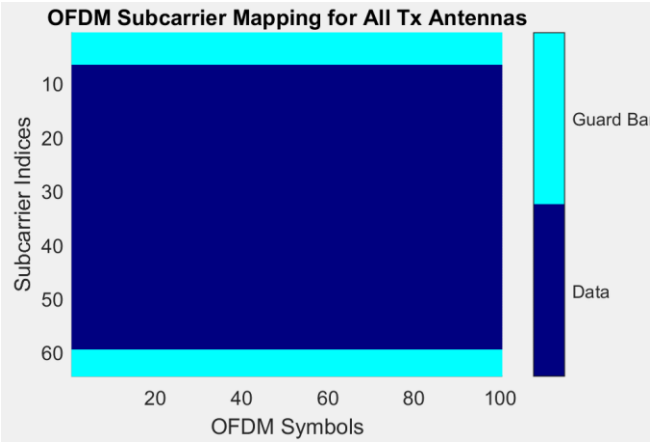

Figure 3. Resource Grid for OFDM waveform (a)

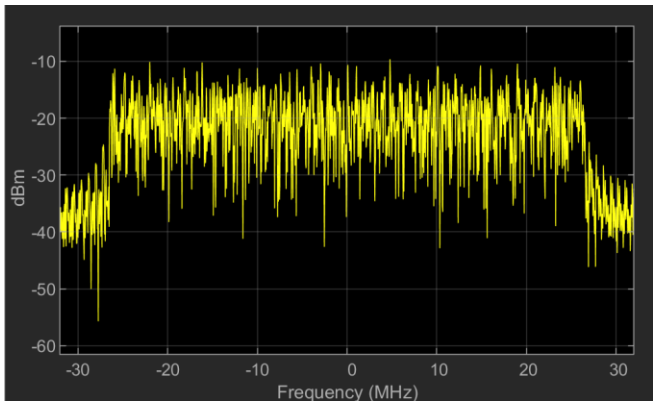

Figure 4. Frequency spectrum for OFDM waveform (a)

As shown in Figure 4, 64 Sub-Carriers are stacked in the ODFM resource grid from which 11 of them act as band guards, and the rest are data sub-carriers. The horizontal axis represents the resource grid in the time domain as OFDM symbols; 100 are displayed as configured in Table 1; this resource grid does not include a DC null nor pilot sub-carriers. Figure 5 shows the frequency spectrum of the generated OFDM signal and can only show the specified signal bandwidth. Fifty-three data sub-carriers (Result of the subtraction of 11 from the initial 64) with 1 MHz sub-carries were defined resulting in a total bandwidth of 53 MHz (Or 64 MHz considering the guard-band).

Parameter	**Value**
FFT Length	128
Guard Band Sub-Carriers	6 and 5
DC Null	Yes
Cyclic Prefix Length	16
OFDM Symbols	100
Sub-Carrier Spacing	1 MHz
Pilot Input	11:12:120

Table 2. Parameter table for OFDM waveform (b).

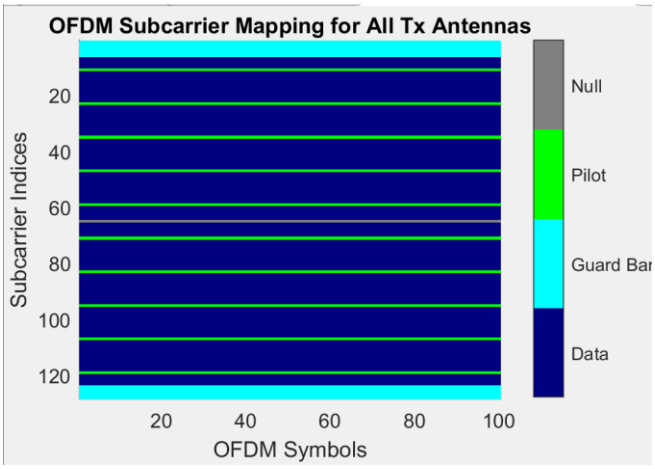

Figure 5. Resource Grid for OFDM waveform (b)

Table 1 shows a different configuration for a second OFDM signal. This new set increases the number of sub-carriers to 128, keeps the original amount of guard-band sub-carriers, includes arbitrarily placed pilots every 12 subcarriers (starting from 11 and ending in 120) and the DC null sub-carrier.

4G LTE

The LTE standard uses OFDM and assigns fixed values to the parameters in the past tables and assigns new special functions to resource elements. The LTE standard features the following parameter values.

Parameter	Value
Sub-Carrier spacing	15 kHz
Symbol time	66.6 μs
Sub-Carriers per Resource block	12
Symbols in a Resource block	7
Sub-Frame duration	0.5 ms
Available BW	1.4, 3, 5, 10, 15, 20 MHz
Available Resource Blocks	6, 15, 25, 50, 75, 100
Duplexing Mode	TDD/FDD

Table 3. LTE standard numerology.

LTE supports two frame structures, one for Frequency Division Multiplexing and the other for Time Division Multiplexing and their arrangement of each frame depends on its duplexing characteristics.

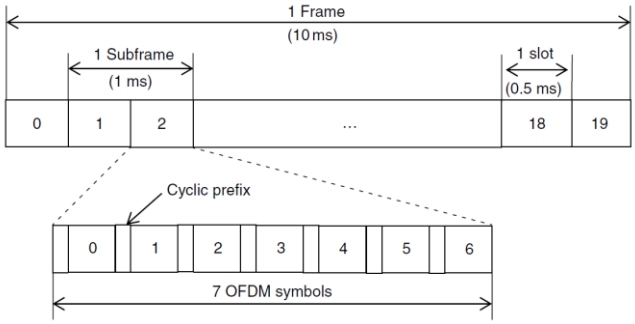

Figure 6. Type 1 frame (FDD)

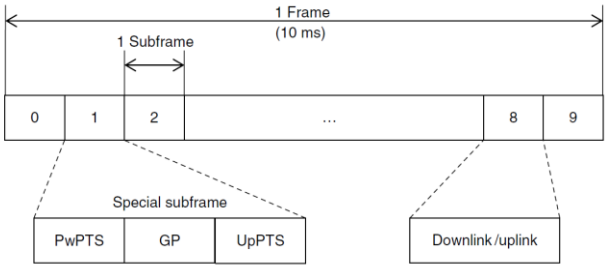

Figure 7. Type 2 frame (TDD)

Both frames may have the following symbols.

- Physical Downlink Shared Channel (PDSCH): User data is transmitted in this channel.
- Primary Synchronization Chanel (PSCH): Used for synchronization in cell search.
- Secondary Synchronization Channel (SSCH): Used to synchronize timing and to transmit cell group ID during a cell search.
- Physical Broadcast Channel (PBCH): Carries cell information.
- Physical Downlink Control Channel (PDCCH): Used for forwarding error correction, resource allocation and Uplink schedule grant.
- Physical Control Format Indicator Channel (PCFICH): Indicates the number of PDCCH symbols per subframe.
- Physical Hybrid ARQ Indicator Channel (PHICH): Carries H-ARQ information.
- Physical Multicast Channel (PMCH): Carries Multicast data.

The following grid was generated in https://www.sqimway.com/lte_resource_grid.html

and outputs a visual reference showing all the resource grid details such as block number, frame number, sub-frame number, symbol and channel type. These grids are also found in the Appendix.

Parameter	Value
Duplexing Mode	FDD
Channel Bandwidth	1.4 MHz
Cyclic Prefix Length	Normal
No. of Tx Antennas	2
MBSN Subframe	None
Physical Layer Cell ID	0
Control Format Indicator	1
PHICH factor	1
PHICH duration	1 Symbol

Table 4. LTE Resource grid setting for FDD frame type.

The resulting LTE resource grid can be seen on this website (Figure 37). This grid shows 6 RBs and half a frame (10 Sub-frames (Half of the total type 1 frame) → 20 slots per frame → 140 symbols per frame). Each sub-frame starts with several PCFICH, PHICH and PDCCH to schedule and configure the contents of the upcoming slots in the given sub-frame. Sub-frames can be dedicated to transmitting user data or synchronization, the latter type can only be seen in sub-frame 0 and 5, and the remaining sub-frames are used for data transmission. In every sub-frame, some symbols are used as a reference of power transmission from an eNode B, and its arrangement depends on the number of Tx antennas and port number.

Parameter	Value
Duplexing Mode	TDD
Channel Bandwidth	1.4 MHz
Cyclic Prefix Length	Normal
No. of Tx Antennas	2
MBSN Subframe	None
Physical Layer Cell ID	0
Control Format Indicator	1
PHICH factor	1
PHICH duration	1 Symbol
TDD Uplink/Downlink Configuration	4 DL, 4 UL and 2 Special Sub-frames
Special Sub-frame Configuration	9 DwPTS symbols and 1 UpPTS symbol

Table 5. LTE Resource grid for TDD frame type.

The resulting LTE resource grid can be seen on this website (Figure 38). This grid uses the type 2 frame (TDD) and shows one frame (10 Sub-frames → 20 slots per frame → 140 symbols per frame) and the contents of these are divided into Downlink, Uplink and Special sub-frames. Like type 1 frame, every downlink sub-frame starts with PCFICH, PHICH and PDCCH channels to schedule and grant resources. Uplink sub-frames are assigned to the UE, and the base station does not define them. Special sub-frames happen between UL and DL sub-frames, allowing synchronization and a guard-time between Ul and DL.

Software Defined Radio

Software Defined Radio (SDR) is a term to refer to radio systems with almost all its functionality done in Software, instead of hardware as it is commonly found in most of the RF applications in recent times. An ideal SDR, as shown in Figure 8, would have an FR Front End only consisting of a power amplifier and high-speed Analogue to Digital converter. At the same time, the remaining physical layer functions such as modulation, synchronization or encoding are done using DSP.

SDR systems are expected to work in a wide range of the frequency spectrum and to perform various operations as a dedicated hardware implementation would have. For example, using a low-cost SDR unit for hearing a local FM radio station and for getting an OFDM signal using QAM modulation in the 2.4 GHz band are both widespread uses.

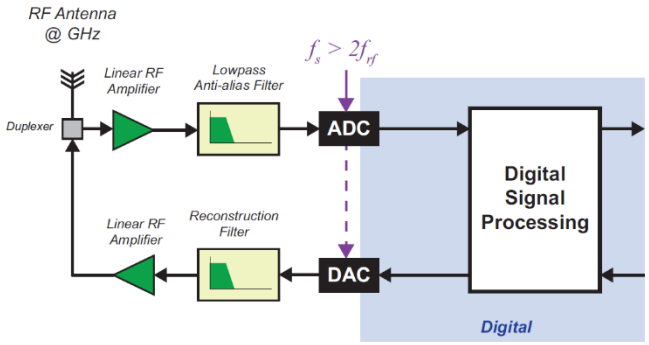

Figure 8. Ideal SDR architecture. [1]

Hardware and Flexibility

Unlike old radio units using specialized hardware to receive and process a particular kind of incoming signal, SDR hardware is generic enough to process data of several frequencies and modulation schemes; an FPGA inside the SDR radio often does this feature. Field Programmable Gate Arrays (FPGA) is a hardware programmable device, instead of software programmable as the commonly known microcontrollers. An FPGA is configured using Hardware Device Language (HDL) that describes the intended behaviour of the FPGA. FPGAs, in the context of DSP, are faster and efficient than microcontrollers; because to the dedicated DSP slices inside the FPGA, the available tools to design and simulate RF systems and the much higher processing speed for RF applications.

The SDR device used for the following sections is the RTL-SDR, a low-cost, receive-only SDR capable of receiving signals up to 1750 MHz which uses a monopole antenna. The SDRSharp software was used to interface with the RTL-SDR.

Mobile Communications Signals

Second, third and fourth generations of mobile communications are still available for people to use, each one of these generations having a particular space in the frequency spectrum. Most of them are available in the range supported by the RTL-SDR.

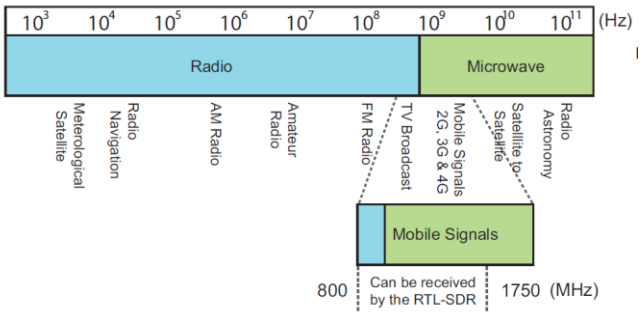

Figure 9. Mobile Cell Signals compared to the RTL-SDR frequency range. [1]

Sadly, neither spectrogram nor frequency response plots will not allow seeing the modulation scheme of any generation. Also, time-domain properties are hard to notice using the SDRSharp software.

2G

The second generation of mobile communications is defined by its multiple access technique: TDMA. Time-Division Multiple Access assigns a time slot to each user to transmit data. These messages are 200 kHz wide and are located in between 890-915 for the Uplink and 935-960 for the Downlink. [1]

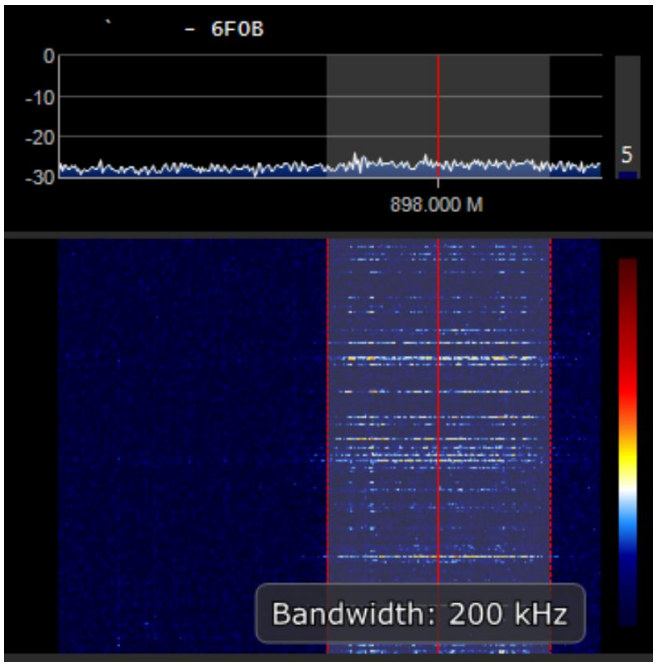

Figure 10. Spectrogram signal from 2G at 898 MHz from the RTL-SDR.

3G

The MA technique of this generation is Code-Division Multiple Access. CDMA is based in the spread spectrum technique, in which many UE can use the same frequency spectrum by spreading their messages using pseudo-random coding. The width of the CDMA spectrum is 5 MHz, which is almost double the RTL-SDR can sample. CDMA is mostly found at 1700 MHz and above, but some signals are still found in the 800-900 MHz range. [1]

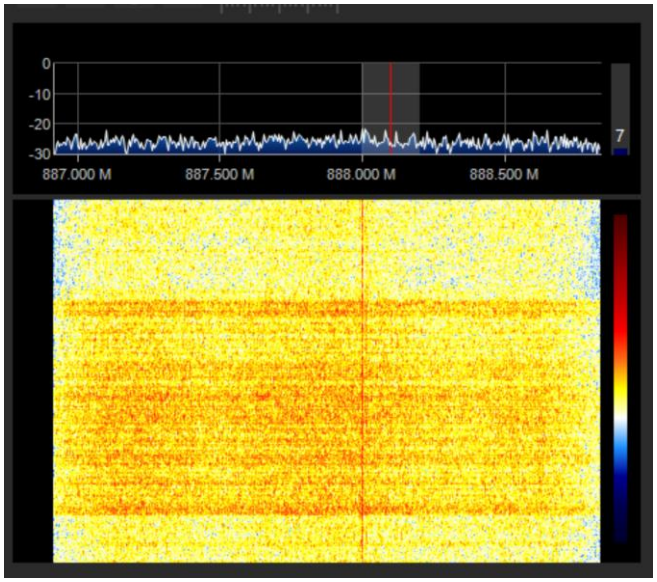

Figure 11. Spectrogram signal from 3G at ~888 MHz from the RTL-SDR

4G

As mentioned in **Wireless Waveforms - OFDM**, the LTE standard supports deployments of 1.4 to 20 MHz, so, probably, the RTL-SDR will not be able to sample the entire spectrum. As LTE uses OFDMA, a multicarrier system is expected to be found while using the SDR unit, specifically sub-carriers with both spacing and width of 15 kHz.

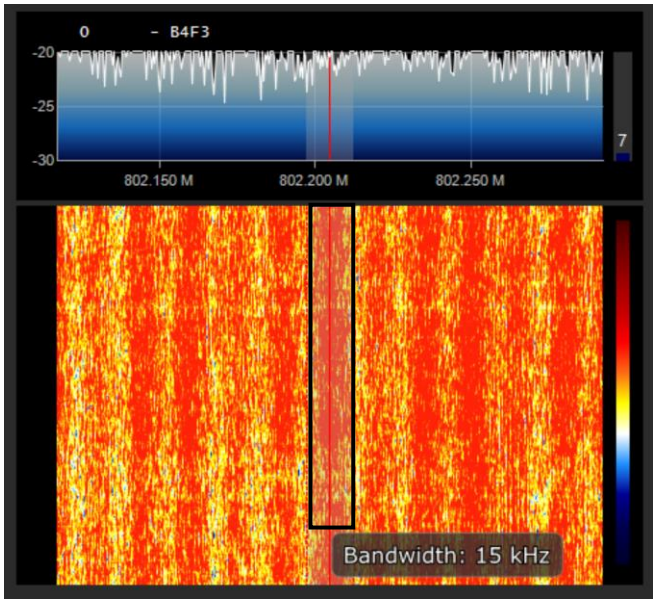

Figure 12. Spectrogram signal from 4G at between 800.5 – 810.5 MHz from the RTL-SDR

mm-Wave

The millimeter-wave (mm-Wave) is the frequency spectrum between 30 and 300 GHz, in which the wavelength of the signals is between 1 and 10 mm. The mm-Wave comes with a much higher path loss attenuation and its inherited properties such as oxygen and water absorption, foliage blockage and precipitation attenuation of the electromagnetic waves. Besides, the mm-wave multipath behaves differently across surfaces; this means engineers must consider rapidly changing channels. Finally, the mm-Wave is not capable of penetrating walls or most solid objects, making signal reception an additional challenge to what has already been discussed. [2, 3, 4]

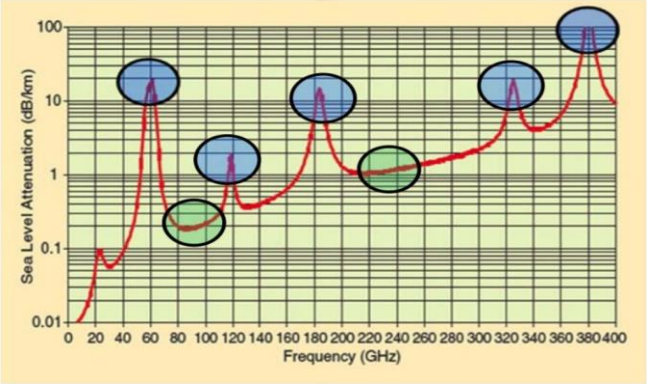

Figure 13. Atmospheric absorption of electromagnetic waves. [2]

Entities such as the 3rd Generation Partnership Project (3GPP), the 5G Channel Model (5GCM), Mobile and Wireless Communications Enablers for the Twenty-Twenty Information Society (METIS) and the Millimeter-Wave Based Mobile Radio Access Network for 5G (mmMAGIC) have developed different models for the mm-Wave in environments such as Urban Macrocell (UMa), Street Canyon (UMi) and Rural Macrocell (RMa) for both Line of Sight and No Line of Sight scenarios. The following simulations use the 3GPP model specified in the 3GPP TR 38.901, which is a document describing the path loss model, its constraints, derivation, and assumptions. [2]

Model	UMa	UMi	RMa
Distance	10 – 5000 m		>1 m
Frequency	0.5 – 100 GHz		73 GHz
BS Height	25 m		0 – 50 m
UE Height	1.5 – 22.5 m		0 – 10 m

Table 6. Model constraints for 3GPP path loss model.

A comparison for each model was made, consisting of the individual comparison of UMa, UMi and RMa environments using both LOS and NLOS scenarios. The model parameters are constrained by the restrictions in Table 6 and were lastly selected, as shown in Table 7.

Model	UMa	UMi	RMa
Distance	10 – 5000 m		
Frequency	6-100 GHz		
BS Height	25 m	10 m	35 m
UE Height	10 m		

Table 7. Model parameters.

The 3GPP model was compared to the Free Space path loss equation, which ideally describes the attenuation a signal experience.

$$PL_{dB} = -20\log_{10}(\frac{\lambda}{4\pi f d})$$

Equation 2. Free Space Path Loss.

As seen in **Error! Reference source not found.**, the free space path loss is the less attenuated model, serving as a baseline for both 3GPP models. For every model, the NLOS scenario is the most attenuated, and the LOS scenario is very similar to the free space path loss, excepting the RMa scenario in which there is a constant 10 dB difference. Different to what is displayed in Figure 13, in any of these simulations the atmospheric impact of on the Path Loss is present. For every scenario, the Path Loss is proportional to f_c^2 and d^2.

Changing the frequency of these models shows similar patterns, only changing the scale of the vertical axis.

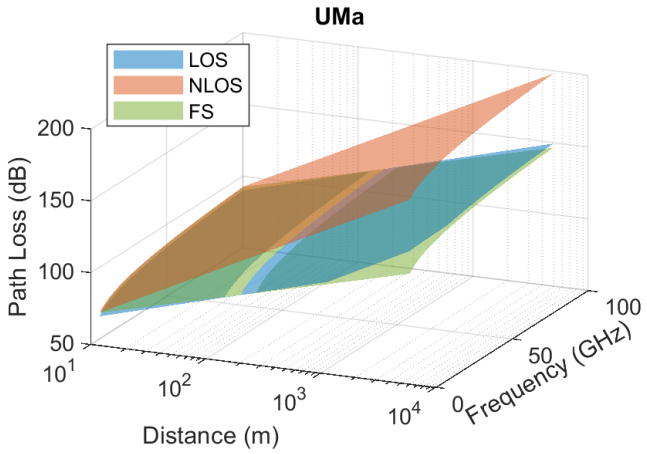

Figure 14. Path Loss for the UMa scenario.

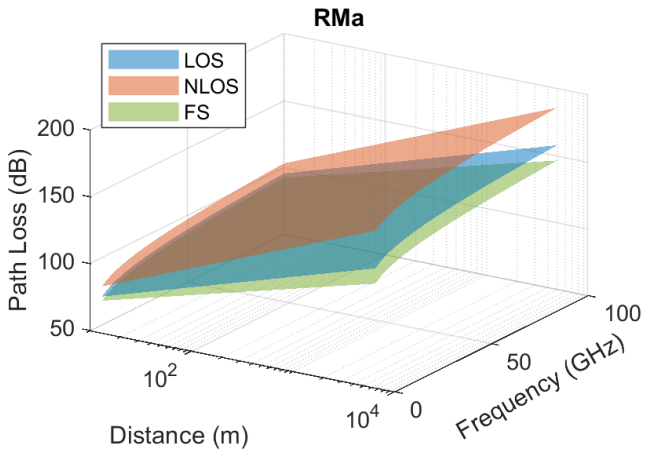

Figure 15. Path Loss for the RMa scenario

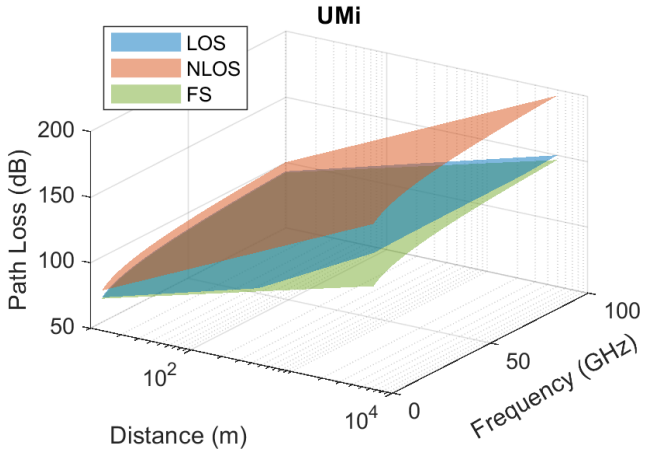

Figure 16. Path Loss for the UMi scenario.

Channel Coding

Chanel Coding describes techniques to correct data that was received incorrectly during transmission over an unreliable channel; these can be classified into Forward Error Correction (FEC) and Automatic Repeat reQuest (ARQ). [1]

- Forward Error Correction: In FEC, a codework (Concatenation of transmitted user data and redundancy) is received and decoded. Decoding can find errors and correct them using the redundant segment of the codeword.
- Automatic Repeat reQuest: ARQ requires a feedback channel from the receiver to transmitter to request retransmission of data in the event of an incorrect reception.

Block Codes

FEC techniques can be classified into Block and Convolutional coding. The main difference between both categories is that convolutional codes are iterative (Or even recursive), and block codes are not. Block Coding uses linear algebra to encode at the transmission and try to get the bits that have been corrupted in transmission. There are many algorithms for encoding using block codes, but all of them are based on the following parameters:

- Codeword Length (N): This is the length of the encoded message. Designers can define this parameter by choosing a positive integer power of two (M).
- Message Length (k): This is the length of the user message to be transmitted. The number of bits to be encoded is given by the codeword length and the parameter M.
- Minimum Distance (d_{min}): This parameter defines the error correction capability (t) of the coding algorithm. It is given by the smallest number of differences between every possible codeword combination.

Depending on the coding algorithm, equations and conditions may differ from one algorithm to another. The equations that relate all these parameters are the following.

	Hamming	Reed-Solomon	Bose-Chaudhuri-Hocquenghem
M	$M \geq 3$	$M > 1$	$M \geq 3$
N	$N = 2^M - 1$		
k	$k = N - M$	$k < n - 1$	$k < m \cdot t + n$
d_{min}	$d_{min} = 3$	$d_{min} = N - k - 1$	$1 > \frac{d_{min}}{2t} > 2$
	$d_{min} = 2t - 1$		

Table 6. Block Coding equations for Hamming, RS and BCH codes. [1]

Performance

The purpose of coding is to enhance BER performance at the cost of data throughput.

$$R = \frac{k}{n}$$

Equation 3. Coding ratio for most linear block codes. [1]

As seen in Equation 3, the coding ratio is linear, unlike the BER relation with the same parameters. Hence, optimization can be done to achieve the best BER in a specific SNR value while getting an acceptable throughput. As a summary, having a low throughput ratio does not translate to high BER performance.

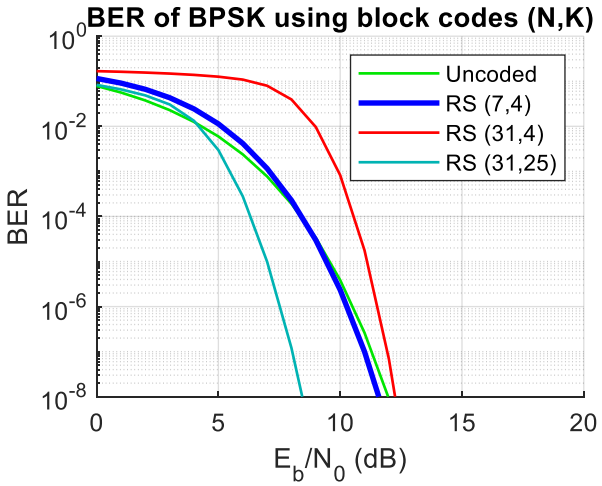

Figure 9. Theoretical BER performances for BPSK over an AWGN channel using linear block coding algorithms.

Simulation

A Simulink model was designed to simulate a single user transmitting encoded data using 8-PSK for Hamming and RS, and QPSK for LDPC over an AWGN channel (Not fading because MATLAB does not offer the theoretical BER plots for fading channels). Three linear block coding algorithms were tested: Hamming, Reed-Solomon (RS) and Low-Density Parity-Check, specifically the later has some simulation constraints such as narrow valid SNR range (According to MATLAB documentation [2], community forums and community files)

Hamming and Reed-Solomon

The first two coding schemes are the simplest ones, both Hamming and Reed-Solomon are linear block codes based on the theory given in **Block Codes**. The model parameters for simulation are the following.

Bernoulli Binary		
Sample Time	0.01 Seconds – 100 Hz	
Samples per Frame	Hamming	57
	RS	52
AWGN Channel		
Eb/No	Defined by BERtool	
Number of bits per symbol	3	
Symbol Period	0.022 Seconds	
Encoders		
N	Hamming	63
	RS	15
k	Hamming	57
	RS	13

Table 7. Model parameters for Hamming and Reed-Solomon simulations.

Values as the sample time for the Bernoulli Binary block are arbitrary since there are no fading conditions to meet. Samples per Frame in the same block is defined by the encoder's input signal constraint being these k and k times m for Hamming and Reed-Solomon, respectively. The remaining parameters in the model are set to their default value.

To define both encoders, arbitrary values for M where given, these being 6 and 4 for Hamming and Reed-Solomon respectively. Values for N and k were assigned by using the equations in Table 6.

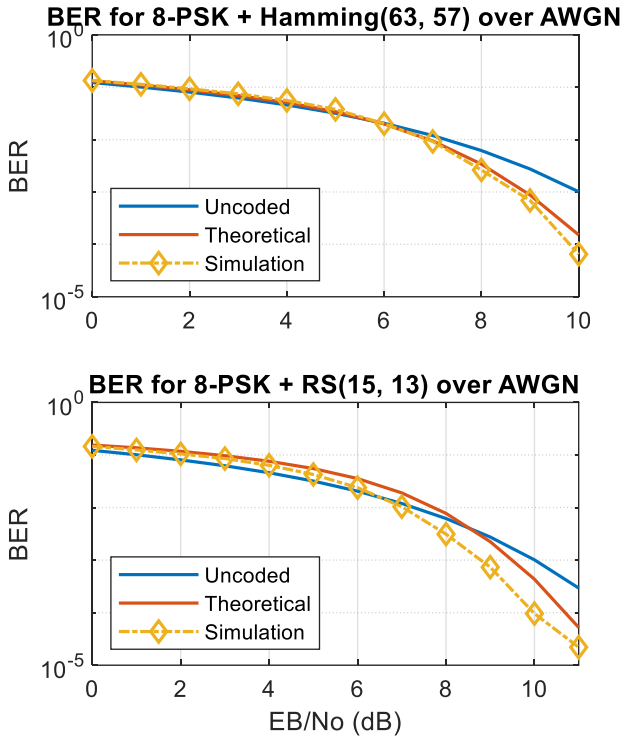

Figure 10. (Up) BER performance for Hamming encoded 8-PSK modulated system over AWGN. (Down) BER performance for Reed-Solomon encoded 8-PSK modulated system over AWGN.

Both models were designed for comparing numerology and performance, having identical detection and correction capabilities ($d_{min} = 3$, $t = 1$); meaning only a single bit can be corrected.

The Hamming encoded plot presents a slightly better BER performance compared to the uncoded scenario when EbNo is higher than 6, due to the probability of having more than one corrupted bit is reduced at this power. The coding rate for this system is ~90%, so no significant BER performance boost is achieved even with the high N and K numbers.

The RS encoded plot presents a worse BER performance at lower EbNo, this is because the amount of parity bits in the codeword is too small, but at EbNo higher than nine a performance boost is achieved. The coding rate for this system is 86%;

hence this system is objectively worse than the last, offering less BER performance and less throughput.

LDPC

Low-Density Parity Code is the FEC algorithm proposed for 5G. It is a linear block code in which both parity bits and message are equally protected, and the parity check matrix is created randomly as a sparse matrix (few 1s and many 0s to increase the Hamming distance). [2]

Bernoulli Binary	
Sample Time	0.01 Seconds – 100 Hz
Samples per Frame	32400
AWGN Channel	
SNR	Defined by BERtool
LDPC Encoder/Decoder	
Parity-check matrix	Dvbs2ldpc(1/2)
Demodulator	
Decision Type	Approximate Log-Likelihood ratio
Noise Variance	1/db2pow(SNR)

Table 8. Model parameters for the LDPC simulation.

The LDPC encoder/decoder in Simulink was only able to work using a different overall configuration of the whole block diagram. AWGN block had to be set to SNR instead of Eb/No and the demodulator block was set to Approximate Likelihood ratio instead of hard detection (As shown in MATLAB's documentation). The remaining blocks have the same parameter values as the Hamming and Reed-Solomon simulations.

This model's parity check matrix is given by the DVB-S2 specification, which consists in an irregular LDPC matrix with 32400 message bits and 64800 total bits, six 1s in the first row and seven 1s in the remaining rows. The code rate for this encoder is ½. [2]

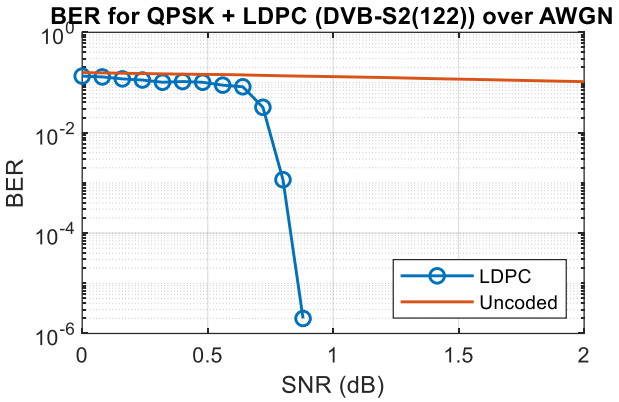

Figure 11. BER performance for Hamming encoded 8-PSK modulated system over AWGN.

LDPC encoder could not output results for SNR higher than 0.8 dB, but when compared to the uncoded plot, the error performance shows to be significantly enhanced.

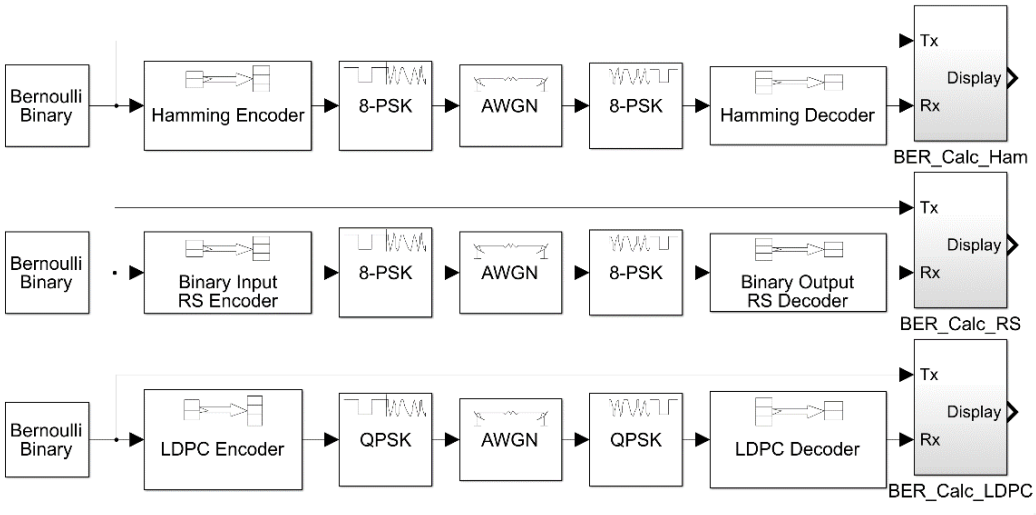

Figure 19. Block Diagram Model for Hamming, Reed-Solomon and LDPC coding.

OFDM

As explained in **Wireless Waveforms - OFDM**, OFDM is the frequency diversity technique used in 4G, based in the use of several low-bandwidth sub-carriers orthogonally placed to increase bandwidth efficiency and avoid channel impairments and frequency selective fading.

For designing a basic OFDM system, parameters such as the number of subcarriers and the job of each one of them (Data, pilot or null/Guard-Band), the modulation scheme (Many schemes can be used for different subcarriers).

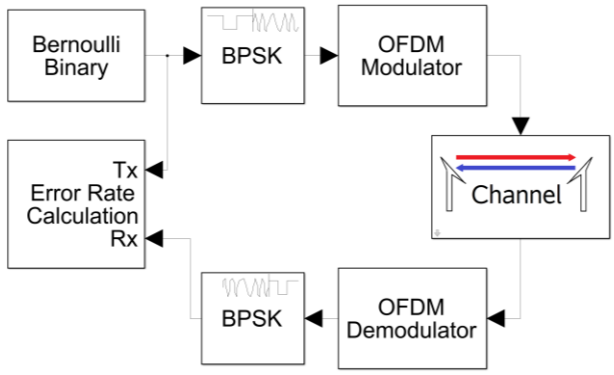

Figure 21. Block Diagram model for OFDM system. The Channel block includes combination of fading and AWGN channels.

Simulation

Three simulations were carried out using the proposed block diagram model; parameters are shown in the following table.

Bernoulli Binary			
Sample Time	0.01 Seconds – 100 Hz		
Samples per Frame	53	1013	65524
OFDM Modulator/Demodulator			
FFT Size	64	1024	65535
Number of Guard Bands	[6 (Lower boundary); 5 (Upper Boundary)]		
AWGN Channel			
EbNo	Defined by BERTool		
Bits per Symbol	53	1013	65524
Symbol Period	0.01 Seconds – 100 Hz		

SISO Fading Channel	
Discrete Path Delays	0.00001 Seconds
Max Doppler Shift	0.001 Hz

Table 11. Model parameters for OFDM simulation.

Settings such as Sample Time/Period in Bernoulli Binary and AWGN Channel were set arbitrarily, the fading channel was configured to be in flat fading, and the remaining parameters in non-mentioned blocks are set to default.

For the first simulation run, default parameter values were used in the OFDM modulator/demodulator (FFT size of 64, 11 guard band subcarriers, no DC null subcarrier and no pilots; parameters such as cyclic prefix length, number of symbols and antennas are not relevant for this simulation). As the input signal, an array of FFT size minus total guard-band sub-carriers is needed to fill each data subcarrier in the OFDM modulator. Since BPSK modulation is being used, only a single bit can be processed at a time, so no compensation is required in the input signal size.

Since OFDM is overly sensitive to Doppler shifting, a fixed low shift was selected for all the simulations being this 0.001 Hz to avoid ISI and get consistent non-ideal results.

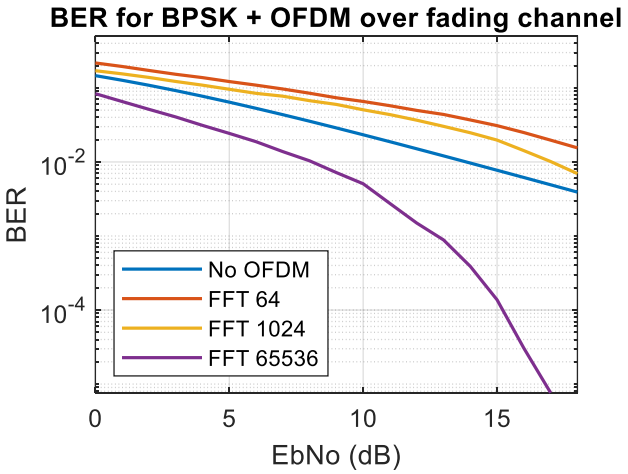

Figure 22. BER performance of OFDM over a Rayleigh channel using different FFT sizes.

As shown in Figure 22, BER performance increases in proportion to the FFT size and even surpasses the theoretical BPSK without OFDM. Although implementing an OFDM system of that size is unpractical, actual systems used in LTE have FFT lengths from 128 to 2048 for 1.25 MHz and 20 MHz, respectively. [5]

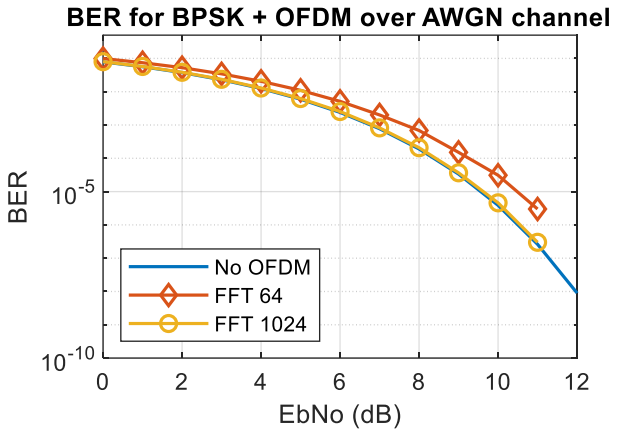

Figure 23. BER performance of OFDM over an AWGN channel using different FFT sizes.

Figure 23 shows the same model but using an AWGN channel instead of fading. The FFT size still enhances BER performance but its capped by the modulation's BER theoretical performance.

Spatial Diversity

Spatial diversity describes techniques related to using multiple antennas for transmitting and receiving; more advanced concepts such as MIMO and massive MIMO are based on this concept. Spatial diversity has several architectures to enhance data throughput, bit error performance or both; these architectures involves adding several antennas at the transmitter or the receiver and the required algorithm to process the data from the additional data streams.

The models and simulations shown in this report have the goal to increase Bit Error Performance.

Rx Diversity

The receive diversity scheme consists in adding several antennas in the receiver side and then select or combine the incoming signals from every antenna. These algorithms are the Selection Combining, Maximum Ratio Combining (MRC) and Equal Gain Combining (EGC).

The most straightforward algorithm is the SC, which only selects the highest fidelity signal from all the antennas. This algorithm may require little channel estimation to decide which antenna to use, but it can be switched arbitrarily. As a summary, this algorithm is the easiest to implement but delivers the weakest performance.

MRC is an algorithm in which the signals coming from every antenna and combines it after multiplying them with their respective channel conditions (h_m). This requirement means that MRC needs precise channel estimation to get a complex representation for both magnitude and phase response of the channel. The received signal from an antenna is given by the following equation.

$$r_m = h_m s_n + n_m$$

Equation 4. Received signal from every antenna.

Where m represents the antenna number, S_n represents the sent message at the instant n and n_m represents the noise profile of the channel. The MRC algorithm equation is given by the following equation.

$$s = \sum_{m=0}^{M-1} h_m^* r_m$$

Equation 5. MRC equation.

After processing the incoming signals, the combined result can be further processed using a Maximum Likelihood Detector algorithm.

A model of this scheme was done using Simulink and is shown in Figure 24.

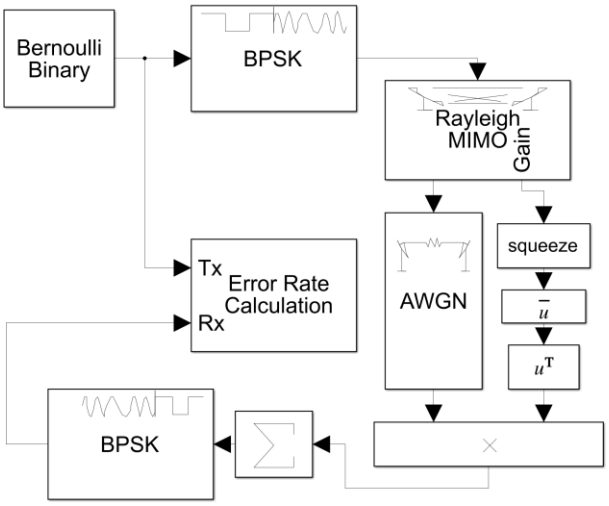

Figure 24. MRC block diagram model.

A simulation was performed using this model, which is an extension of a standard 1x1 wireless communications system model. The most significant differences are the MIMO fading channel block, which holds the same fading parameters while adding the number of antennas at transmitter and receiver. Besides, the MRC algorithm is performed by the conjugation, product, and sum of elements blocks; as seen in Equation 5. As the gain channel in the MIMO fading block is a 4-dimensional matrix with redundancies, a squeeze block is used to get the parameter channels as a matrix with dimensions Rx times Tx.

The parameters not mentioned in the previous paragraph are set as a default or a commonly known parameter.

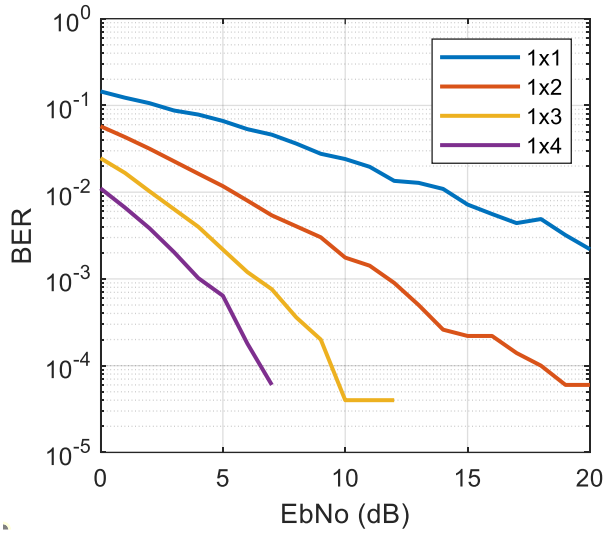

Figure 25. BER performance for Rx diversity using the MRC algorithm.

As shown in Figure 25, BER performance is enhanced by adding more receive antennas. Since the most considerable gap in performance is between 1x1 and 1x2, it is implied that adding more antennas do not add a liner increase in performance. Hence, studies and simulations must be done to intelligently design a spatial diversity application that is both high-performance and cost-efficient.

Tx Diversity

The Tx diversity adds multiple antennas at the transmitter side and then apply a space-time coding algorithm; the one reviews is known as the Alamouti code. This technique is based on the resulting addition of signals at the receiver due to the multipath properties of the channel, as it assumes the worst-case condition in which the addition is always destructive. The space-time part of the algorithm is to send two messages (S_0 and S_1) over two antennas, the first antenna sends S_0 and the second antenna send S_1. Then, the same two messages are sent, but using different antennas and phases; the first antenna sends $-S_1^*$ and the second antenna sends S_0^*.

$$r_0 = h_0 S_0 + h_1 S_1 + n_0$$
$$r_1 = -h_0 S_1^* + h_1 S_0^* + n_1$$

Equation 6. System of equations for Alamouti Space-Time coding.

Once two equations are given, the contents of the message can be estimated using simple algebra. These equations can be extended to be used for more messages and antennas; the proportion of used Space-Time coding combinations is called Rate.

Since Space-Time coding is a commonly used feature in wireless communications, Simulink provides a library for this in the Communications Toolbox. By using these blocks, the algorithm can be easily implemented in models for simulations.

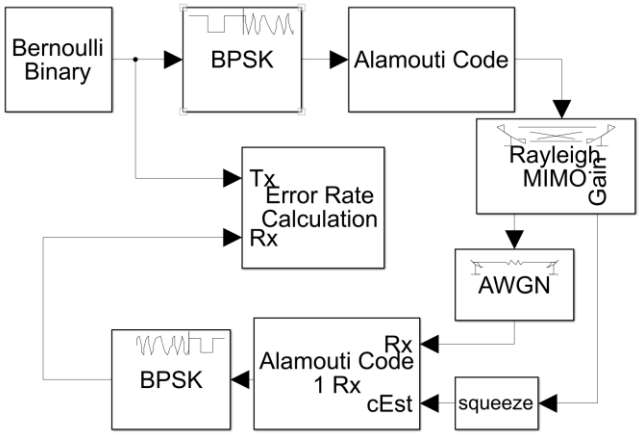

Figure 26. Block diagram model for Alamouti Space-Time coding.

The simulation, similar to the Rx Diversity model, consists of a conventional wireless communications system model, only adding the MIMO fading channel and the Space-Time coding block from the communications toolbox. The number of transmitting antennas is changed to see the impact of this parameter in BER, while the number of receiving antennas is fixed to one. The parameters required for the Space-Time encoder and decoder to work is the number of Tx and Rx antennas and the coding rate, this last being set to ¾ (3 messages in 4 instants) for the simulations for 2 and 3 Tx antennas. The channel conditions and the remaining block parameters are set as default or to a value that makes the model meet its mathematical requirements.

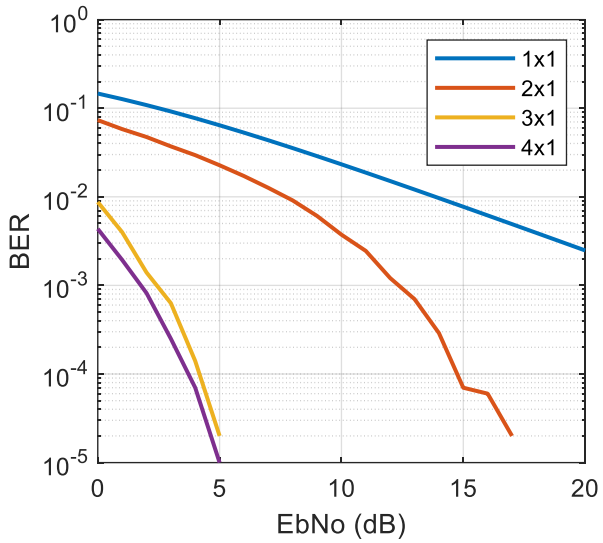

Figure 27. BER performance for Tx diversity using the Alamouti Space-Time coding.

As seen in Figure 27, the BER performance is enhanced as more antennas are added to the system. Unlike Rx diversity, similar improvements can be seen in 2 and 3 transmitter antennas, while a minor one is noticed when adding the fourth antenna.

MIMO

Multiple-Input Multiple-Output is a spatial diversity technique that involves having several antennas at both receiver and transmitter to acquire the same performance benefits that spatial diversity offers. An advanced deployment of this, called Massive MIMO will be used in 5G systems, increasing the number of antennas in base stations from around 10-20 to hundreds [8], allowing multiple simultaneous users and increased throughput and BER performance, while also implementing other techniques such as Beamforming and Full-duplexing to avoid interference and allow better performance when communicating over the mm-Wave spectrum. The current record of highest bandwidth efficiency is 145.6 bps/Hz, achieved using a 128 Massive MIMO array. [9]

Multi-User MIMO

MU-MIMO consists on having several data streams in a multi-antenna system, where the number of antennas at the transmitter side constraints the number simultaneous data streams for every user and the number of antennas at the receiving side must be equal or higher than the number of transmitting antennas. Same as Spatial Diversity, the ratio between Tx and Rx antennas increase both BER and throughput, instead of a tradeoff as Spatial Diversity does; but only BER performance will be displayed as a performance metric.

Channel estimation is needed to get an overall combination of all the signals from the receiving antennas, and this is done by merely solving the matrix representation of the incoming signals.

$$\boldsymbol{R} = \boldsymbol{HS} + \boldsymbol{N}$$
$$\boldsymbol{H}^{-1}\boldsymbol{R} = \boldsymbol{S} + \boldsymbol{H}^{-1}\boldsymbol{N}|_{\boldsymbol{N}=0}$$
$$\boldsymbol{S} \approx \boldsymbol{H}^{-1}\boldsymbol{R}$$

Equation 7. MIMO Signal combining.

Where **R** is the received signal matrix, **H** the channel gains for every Tx and Rx antenna combination and **S** is the transmitted signal. In case the number of Tx and Rx antennas is not equal, the inverse of matrix H will not be directly obtainable, and the pseudo-inverse algorithm must be used instead.

The model in Figure 29 represents a 3-user MIMO system in which a total of 9 data streams are assigned unequally to each user.

User	Data Streams
1	4
2	3
3	2

Table 12. Datastream assignment per user.

Each user's data is modulated and then concatenated into a single vector for every antenna to be used in the MIMO fading channel. After adding noise to all the received signals, the estimation algorithm is used to convert from a vector with as elements as Rx antennas to a vector with as elements as data streams. Finally, each user's data streams are separated, demodulated and compared.

The transposition blocks after concatenation and before de-modulation are used to satisfy model compatibilities instead of mathematical requirements.

Simulations were carried out variating the number of receiving antennas, increasing them for each user to have an additional antenna every new simulation. The number of antennas was 9, 12 and 15 receiving antennas.

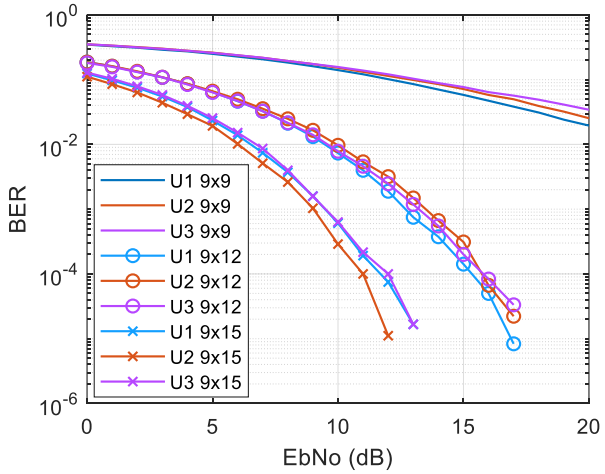

Figure 28. BER performance for MU-MIMO.

The simulation shows two main characteristics. The first one is that every user has similar BER performances in every scenario. The second is that

adding the first additional antenna per user as in the 9x12 scenario enhances the BER performance, while the 9x15 scenario shows a more modest performance difference.

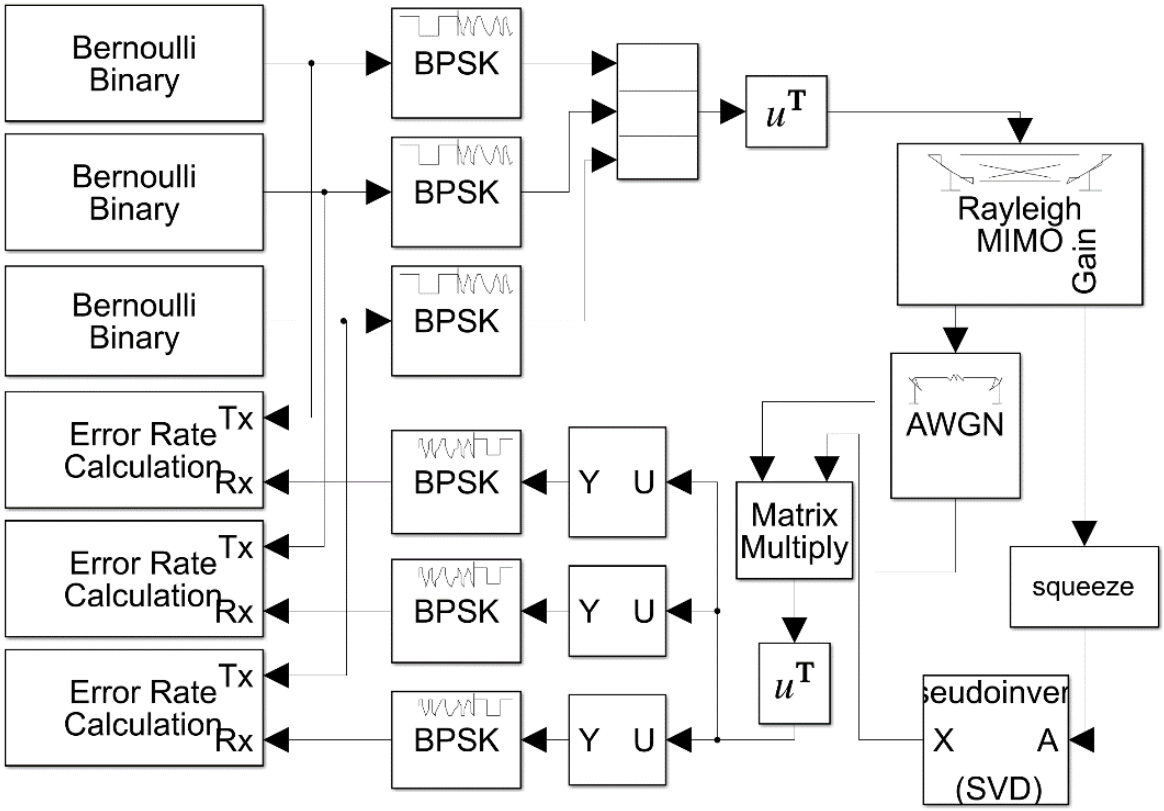

Figure 29. Multi-User MIMO simulation model.

Beamforming

Beamforming is widely used in several fields such as signal processing, radar (sonar) or biomedical. As for mobile communications, Beamforming is used to transmit or receive signals over an antenna array optimally, and it has been considered for the 5th generation of mobile communication systems and was recently included in the IEEE 802.11ax standard (Commonly called WIFI6) as a main feature. Beamforming allows the transmitter to focus power into a specific direction and receiver to only expect signals from a specific direction, without considering the remaining incoming signals.

Beamforming is done by placing an antenna array consisting of several equally spaced omnidirectional antennas, the shape of this array result in the capabilities and performance of the beamforming system.

Beamforming in 5G

5G goals are to enhance data throughput, drastically reduce latency and increase the number of simultaneous users. These goals will be achieved by using the so-called millimetre wave spectrum (mm-Wave) which is defined as the frequency spectrum with a wavelength between 1 and 10 mm, and this spectrum has a range between around 30 and 300 GHz. As of today, most of the available commercial solutions involving RF are located in the sub 6 GHz spectrum; this means using the mm-Wave spectrum is a significant improvement that comes with several engineering challenges such as to design cost-effective hardware capable of generating and processing super-high frequencies and develop techniques for avoiding the natural constrains the mm-Wave has in terms of channel characteristics.

For example, the attenuation due to gas absorption (Pathloss) for a 60 GHz signal is around 10 dB/km, while a 700 MHz signal path loss is around 0.1 dB/km [10]. This only means that for using the mm-Wave and achieve all the goals 5G proposes, a highly efficient transmission and reception scheme is needed only for being able to communicate over the mm-Wave.

Beamforming at the Receiver

The purpose of applying a receiving beamformer is to get signals from the desired direction without getting as much interference from other sources as a single omnidirectional antenna; this is called the combiner stage. Assuming a linear antenna array such as the one represented in Figure 30, an upcoming signal with angle θ would arrive first to X_0 and then to X_1 after a few instants, this lapse is represented as τ which remains constant for all antenna elements.

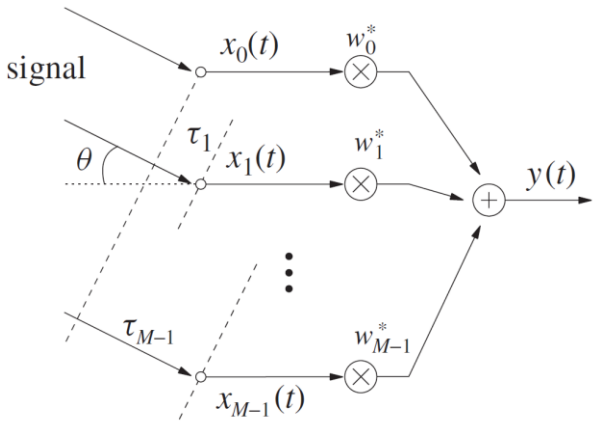

Figure 30. A general structure for the combiner stage at the receiving beamformer. [11]

$$\tau = \frac{d \cdot sin(\theta)}{c}$$

Equation 8. Arrival time difference from one antenna element to the following. [11]

$$y(t) = \sum_{m=0}^{M-1} x_m(t) w_m^*$$

Equation 9. The received signal from the antenna array. [11]

Equation 9 describes the received signal before demodulating using the carrier frequency using combining weights (w_m). For this, the signal X_m (the received modulated signal) is expressed as a phasor for more accessible mathematical analysis, and then Equation 9 is simplified into Equation 11.

$$x_m(t) = e^{j\omega(t-\tau_m)}$$

Equation 10. Phasor representation of the input signal from the antenna element. [11]

$$y(t) = e^{j\omega t} \sum_{m=0}^{M-1} e^{-j\omega\tau_m} w_m^*$$

Equation 11. Received signal from antenna array using phasor notation. [11]

Furthermore, the response of the beamforming system and matrix expression are given by the following equations.

$$P(\omega,\theta) = \boldsymbol{w}^H \boldsymbol{d}(\omega,\theta)$$
$$\boldsymbol{w} = [w_0 \quad w_1 \quad \dots \quad w_m]^T$$
$$\boldsymbol{d}(\omega,\theta) = [1 \quad e^{-j\omega\tau_1} \quad \dots \quad e^{-j\omega\tau_{M-1}}]^T$$

Equation 12. Array response using vector notation.

Like Digital Signal Processing theory, aliasing can affect beam directivity by placing the antenna elements farther away. Hence, the elapsed time between two elements receiving the same message is too large, and the message's direction of arrival cannot be estimated. For a constant distance, the following equation describes the elapsed time of arrival between antenna elements.

$$\tau_m = m\,\tau = m\frac{d\sin(\theta)}{c}$$

Equation 13. Time constant definition assuming constant distance and Direction of Arrival. [11]

$$x_m(t) = e^{j\omega(t - m\frac{d\sin(\theta)}{c})} = e^{j\omega t} e^{-\frac{j\,m\,2\pi\,d\,sin(\theta)}{\lambda}}$$

Equation 14. The received signal from each antenna element considering constant distance and Direction of Arrival. [11]

Moreover, applying the Nyquist Theorem to avoid spatial aliasing.

$$d \le \frac{\lambda}{2}$$

Equation 15. Condition for avoiding spatial aliasing. [11]

$$x_m = e^{j\omega t} e^{-j\,m\,\pi\sin(\theta)}$$

Equation 16. The received signal from each antenna element considering the condition for avoiding spatial aliasing. [11]

$$P(\omega,\theta) = \sum_{m=0}^{M-1} e^{-j\,m\,\pi\sin(\theta)} w_m^*$$

Equation 17. Antenna array response considering condition for avoiding spatial aliasing and Direction of Arrival. [11]

Where sin(θ) can be taken as the normalized frequency (Ω) for design and simulation purposes as the antenna array can be modelled as a low pass FIR filter.

This equations and theory are for Narrowband Beamforming, in which the bandwidth of the incoming signal is not very large. Beamformers are categorized depending on their Fractional Bandwidth (FB); a narrowband beamformer may have a FB lesser than 1%. [12]

$$FB = \frac{f_H - f_L}{(f_H + f_L)/2} = \frac{BW}{f_C} < 1\%$$

Equation 18. Narrowband condition. [12]

For example, a 5 GHz carrier (f_C) could transmit a signal with 50 MHz as bandwidth.

Beamforming at the Transmitter

All the previous equations and theory for the combiner stage is applicable for the precoder stage as well. Only a few differences in concept abstraction appear in theory behind distancing each antenna element in the linear array such as naming renaming w_m as the precoder weights. While having many closely aligned antenna elements improves the performance of the receiving beamformer, at transmission having this situation diminishes the contribution of each antenna and the whole array behaves as a single omnidirectional antenna element.

Increasing the distance between antenna elements reduces the transmitted power in specific directions while maintaining constant power at the direction perpendicular to the antenna array, this is called directivity enhancement. A critical point is placed at half the wavelength of the carrier frequency (λ/2); spacing each antenna element at a distance of λ/2 will enhance directivity without generating secondary lobes while using a distance greater than

λ/2 will still enhance directivity while also generating secondary lobes orientated parallel to the antenna array.

Creating secondary lobes is often an undesired consequence of over separating antenna elements. However, it is a design constrain when a finite and little amount of antenna elements can be placed in the array; this can be solved by:

- Reducing the distance between elements: This will decrease directivity while reducing the power of secondary lobes. A balance can be reached between these two parameters.
- Increasing the number of elements in the array: More secondary lobes will be generated, but all of them with lower power and higher directivity.
- Modifying carrier frequency: Increasing the wavelength to the desired value can have the same result as reducing space between elements.
- Applying a window tapper: Window functions, such as the ones used in DSP systems, are useful for reducing the power of secondary lobes. Commonly used algorithms such as Hamming, Hanning, rectangular or Chebyshev windows may be implemented for beamformers.

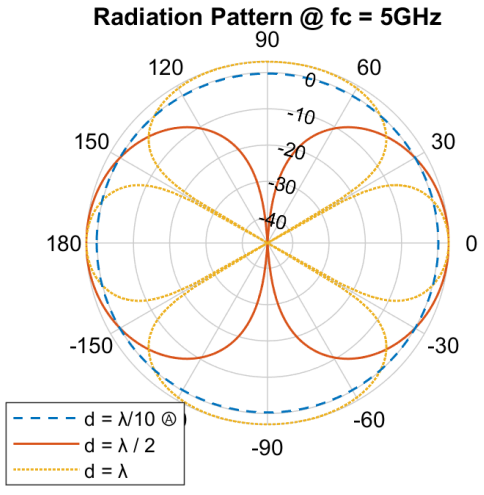

Figure 31. Radiation Pattern for an antenna array with two elements (M = 2) placed at different distances at a carrier frequency of 5 GHz.

Figure 31 shows how changing spacing distance can affect the radiation pattern from making the array behave as an omnidirectional antenna to enhancing directivity and generating secondary lobes.

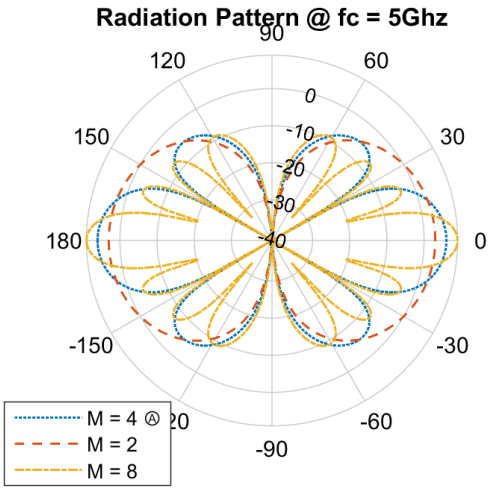

Figure 32. Radiation Pattern for an antenna array with multiple elements placed at a constant distance of λ/2 at a carrier frequency of 5 GHz.

Figure 32 shows how increasing the number of antenna elements in the array can improve the directivity of the main beam by adding several low power lobes.

Types of Beamforming

As stated before, Beamforming has been widely studied, and many forms of techniques and implementations are available now for many different applications. The main category of techniques is the beamformer architecture type, which can be analog, digital or hybrid (Analog-Digital). Each type has its benefits and disadvantages, as well as individual performance.

Digital Beamforming

This type of beamformer is the "simplest" design and mainly relies on a baseband processor to generate the phased output signal already described. The main advantage is that a single design pattern can be followed to create a beamformer; this means a combination of RF chain and power amplifier is required to drive each antenna. That combination is implemented as antennas are needed.

This feature also causes the main disadvantage of digital Beamforming. Having a whole RF frontend to drive a single antenna is highly inefficient and poorly cost-effective since precoding and combining are done in a DSP processor, and each RF frontend have considerable power requirement [13]. Digital beamforming also allows multiuser MIMO and higher spatial diversity.

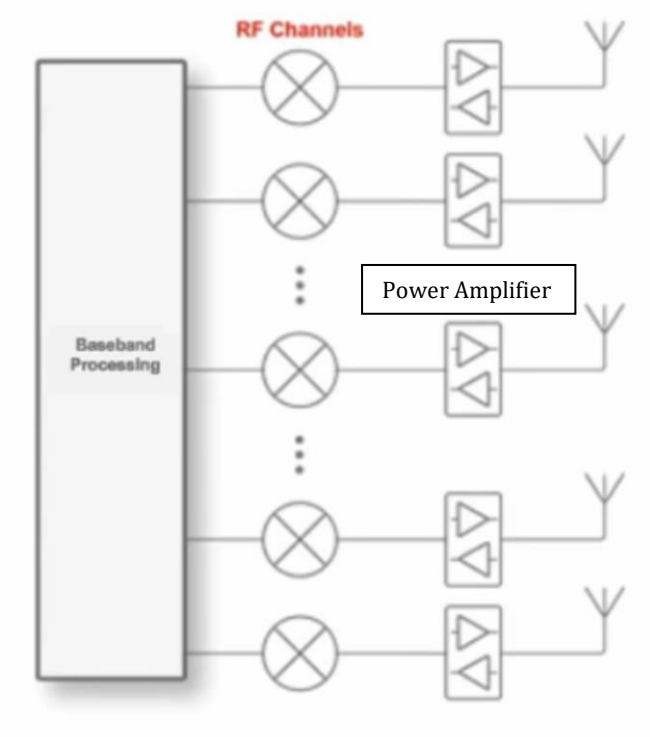

Figure 33. Digital Beamforming block diagram. [13]

Analog Beamforming

This type of Beamforming keeps the processor from phasing and amplifying the output signal by adding an intermediate block between the power amplifier and the RF chain containing a phase and amplitude modifier. Adding this stage allows output signals to be precoded and combined by specified hardware, allowing having a single RF frontend for many antennas and reducing power consumption from the DSP processor.

A disadvantage of this type of beamformer is the added complexity of tuning both hardware and software whenever modifications are needed. Since beamforming parameters are fixed multiuser MIMO and higher spatial diversity are restricted.

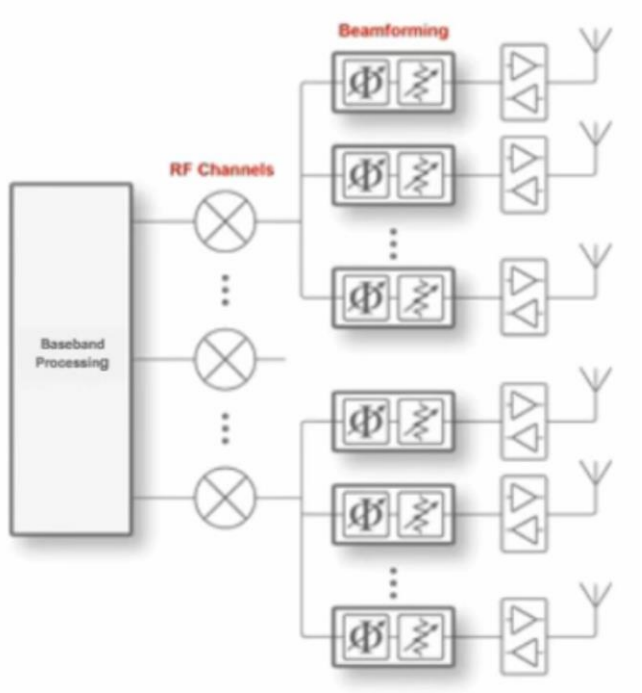

Figure 34. Analog Beamforming block diagram. [13]

Hybrid Beamforming

Hybrid Beamforming combines the advantages of Digital and Analog Beamforming and a few disadvantages. It consists of performing the precoding and combining stages at both DSP processor and RF frontend. This combination allows having the flexibility, multiuser and higher spatial diversity of Digital Beamforming, the high cost and power efficiency and less complicated hardware architecture from Analog Beamforming at the cost of slightly higher power consumption than analog Beamforming and much more complex precoding/combining algorithms.

Beam Steering

Beamformers can change their radiation pattern in order to rotate the main lobe and secondary lobes for avoiding known interference or focus in the desired direction dynamically. Beam Steering can be done in both main or secondary lobes independently to focus and avoid upcoming waves.

A second weight must be added to the precoder or combinator weights to shift the Direction of Arrival and steer the main beam.

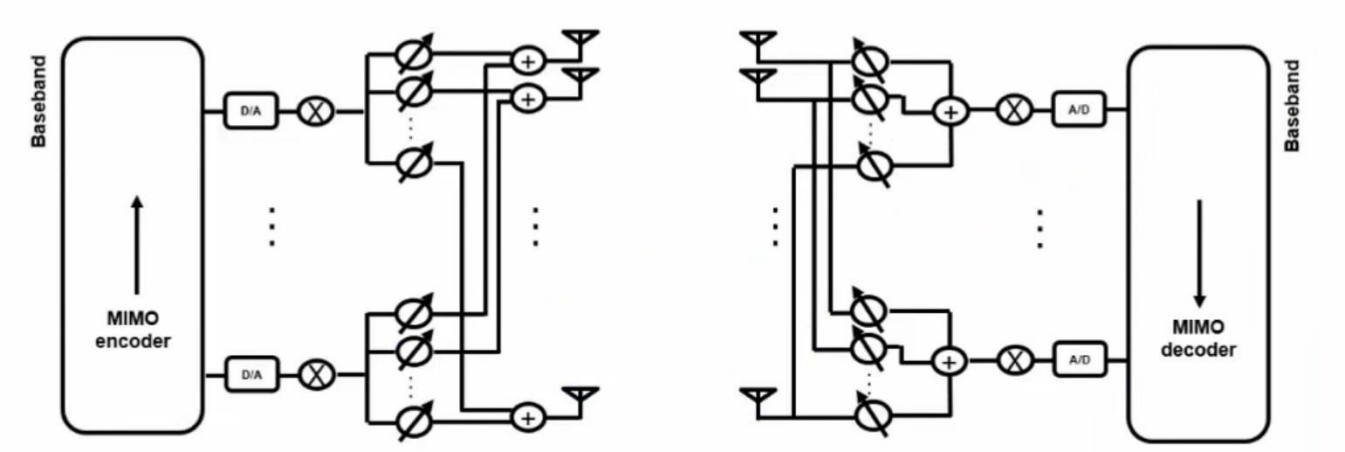

Figure 35. Hybrid Beamforming block diagram. [13]

$$P(\omega,\theta) = \sum_{m=0}^{M-1} e^{-j\,m\,\pi\sin(\theta)} w_m^* S_0^*$$

Equation 19. Antenna array response considering beam steering.

$$S_0 = e^{-jm\pi\sin(\phi)}$$

Equation 20. Steering Vector.

Where φ is the angle of steering (Direction of Arrival/Departure).

The following example shows a Radiation Pattern of a beamformer (Can be either Tx or Rx) consisting in a 5-element uniform linear array (d = λ/2) pointing to the directions ±15° with a Direction of Arrival/Departure of 30 degrees. This beamformer was modelled as a 4th order FIR low pass filter and designed in MATLAB's Filter Designer app, and its normalized passband and stopband were set to sin(5°) and sin(30°), respectively; bandpass weight was set to 1 while stopband was set to 0.5.

MATLAB generated the filter coefficients using the Filter Designer. Then, the steering vector was calculated using Equation 20 and φ = 30. Both are shown below.

$$w_m = [0.120 \quad 0.240 \quad 0.300 \quad 0.240 \quad 0.120]$$
$$S_0 = [1 \quad -j \quad -1 \quad j \quad 1]$$

Finally, the radiation pattern is obtained using Equation 19.

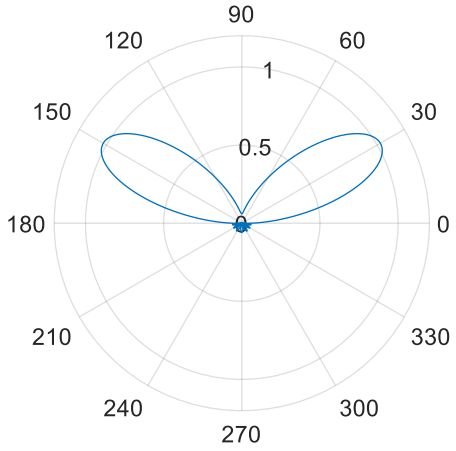

Figure 36. Radiation Pattern, for the example beamformer.

Appendix

Repository

The MATLAB and Simulink simulation files used in the previous sections are available in the following Repository.

https://github.com/JoseAmador95/UoS_TiWC

LTE Grids

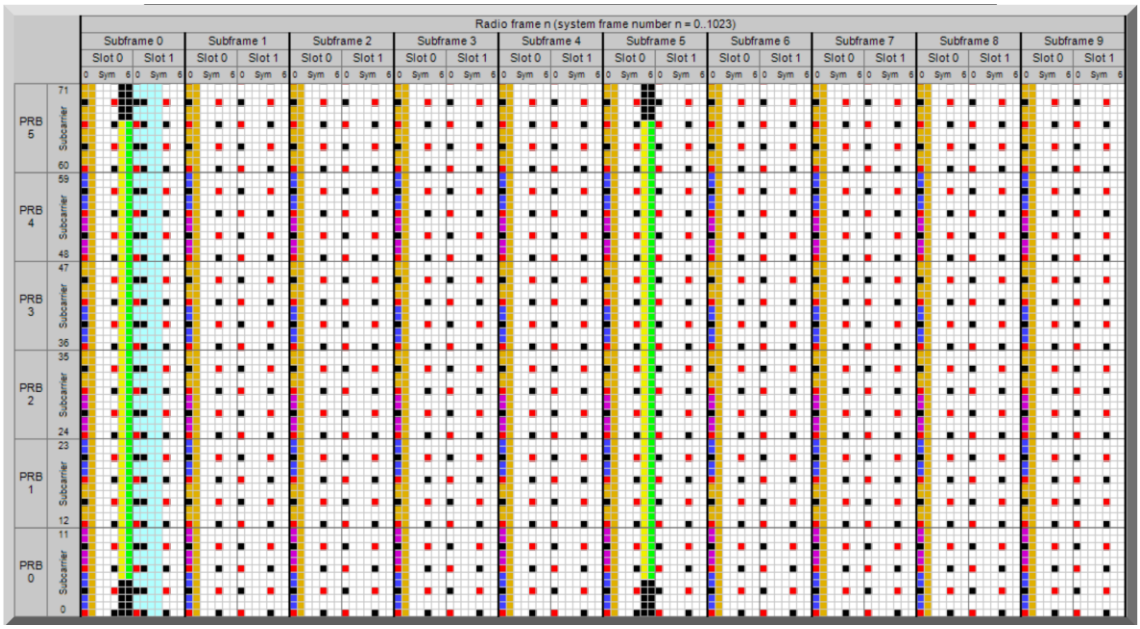

Figure 37. FDD LTE Grid

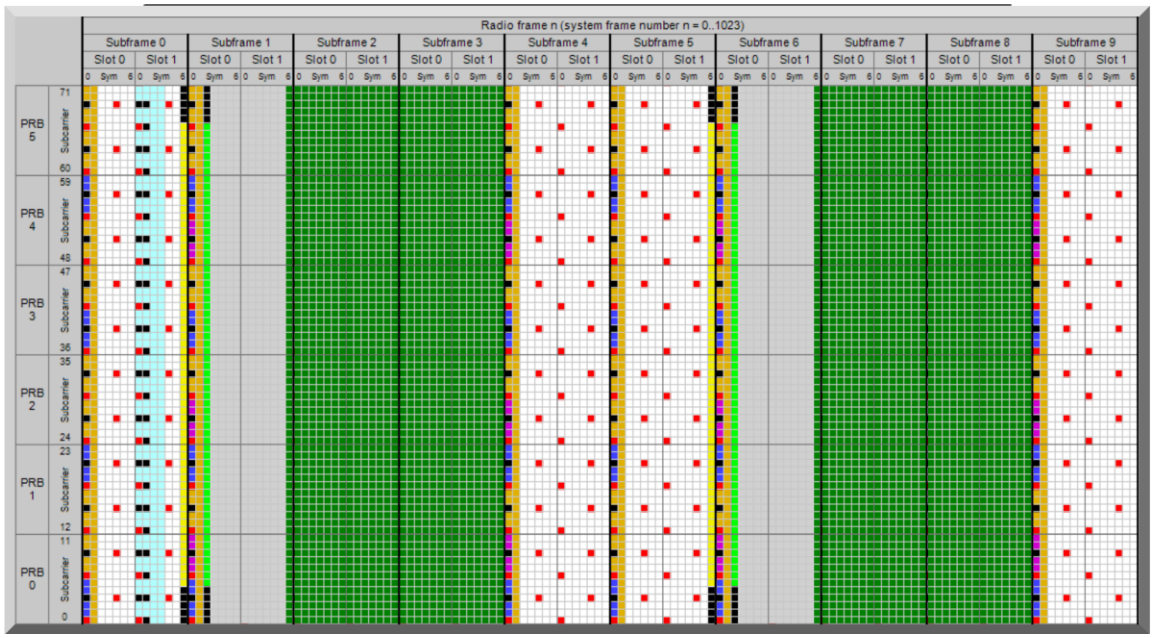

Figure 38. TDD LTE Grid

References

[1] B. Stewart, K. Barlee, D. Atkinson and L. Crockett, Software Defind Radio Using MATLAB & Simulink and the RTL-SDR, Strathclyde Academic Media, 2017.

[2] T. S. Rappaport, G. R. MacCartney and E. Mellios, "Overview of Millimeter Wave Communications for Fifth-Generation (5G) Wireless Networks - With a Focus on Propagation Models," *IEEE Transactions on Antennas and Propagation Vol. 65. No. 12,* pp. 6213-6230, December 2017.

[3] A. Nordrum and K. Clark, "5G Bytes: Millimeter Waves Explained," IEEE, 6 May 2017. [Online]. Available: https://spectrum.ieee.org/video/telecom/wireless/5g-bytes-millimeter-waves-explained. [Accessed 5 May 2020].

[4] Federal Communications Commission, "Millimeter Wave Propagation: Spectrum Management Implications," July 1997. [Online]. Available: http://transition.fcc.gov/Bureaus/Engineering_Technology/Documents/bulletins/oet70/oet70a.pdf. [Accessed 5 May 2020].

[5] K. Haesik, "Wireless Channel Impairment Mitigation Techniques," in *Wireless Communications Systems Design*, 1st ed., Wiley, 2015, pp. 75-122.

[6] A. Grami, "Error-Control Coding," in *Introduction to Digital Communications*, Elsevier, 2016, pp. 433-435.

[7] MathWorks, "MATLAB/Simulink Help Center," MathWorks, 2020. [Online]. Available: https://www.mathworks.com/help/index.html. [Accessed 17 03 2020].

[8] N. Amy and C. Kristen, "5G Bytes: Massive MIMO Explained," IEEE, 17 August 2017. [Online]. Available: https://spectrum.ieee.org/video/telecom/wireless/5g-bytes-massive-mimo-explained. [Accessed 4 May 2020].

[9] N. Amy, "5G Researchers Set New World Record For Spectrum Efficiency," IEEE, 12 May 2016. [Online]. Available: https://spectrum.ieee.org/tech-talk/telecom/wireless/5g-researchers-achieve-new-spectrum-efficiency-record. [Accessed 4 May 2020].

[10] Mathworks, "Hybrid Beamforming for Massive MIMO Phased Array Systems," 2020. [Online]. Available: mathworks.com/campaigns/offers/hybrid-beamforming-white-paper.html?s_iid=doc_wp_AR_footer. [Accessed 12 April 2020].

[11] W. Lui and S. Weiss, "Introduction," in *Wideband Beamforming: Concepts and Techniques*, Wiley, 2010, pp. 1-18.

[12] B. Allen and M. Ghavami, "Narrowband Array Systems," in *Adaptive Array Systems*, Chichester, Wiley, 2005, pp. 32-54.

[13] Peregrine Semiconductor, "Analog Beamforming—What is it and How Does it Impact Phased-Array Radar and 5G?," YouTube, 17 Febraury 2017. [Online]. Available: https://www.youtube.com/watch?v=l4OwU1p8_tE&t=307s. [Accessed 11 April 2020].

[14] W. Tomasi, Advanced Electronic Communications, Error Performance ed., Harlow: Pearson, 2014, pp. 101-106.

[15] 5G Learning, "A Detailed Introduction to Beamforming," YouTube, 6 May 2018. [Online]. Available: https://www.youtube.com/watch?v=HKpQP8H4JRc. [Accessed 7 April 2020].